Journal of Membrane Science & Research

journal homepage: www.msrjournal.com

Research Paper

A New Approach for Fabricating Thin Film Nanocomposite Membranes via a Real-Time Casting/Coating Method

Parisa Daraei *, Kiana Rostami, Farzad Nasirmanesh

Department of Chemical Engineering, Kermanshah University of Technology, 67156 Kermanshah, Iran

Article info

Received 2023-05-07
Revised 2023-07-28
Accepted 2023-08-29
Available online 2023-08-29

Keywords

Real-time casting-coating (RTCC)
Thin film nanocomposite (TFN)
Chitosan
Cellulose nanocrystal
Polyethersulfone

Highlights

- Real-time casting/coating (RTCC) was innovatively examined to prepare membranes.
- A double-layered membrane was achieved with a nanocomposite top layer.
- Two hydrophilic nanofillers i.e. CNC and CNP were applied as modifiers.
- Nanofillers in the top layer were preferred to the mixed matrix membranes.
- The TFN membranes prepared via RTCC showed high flux and efficient dye removal.

Graphical abstract

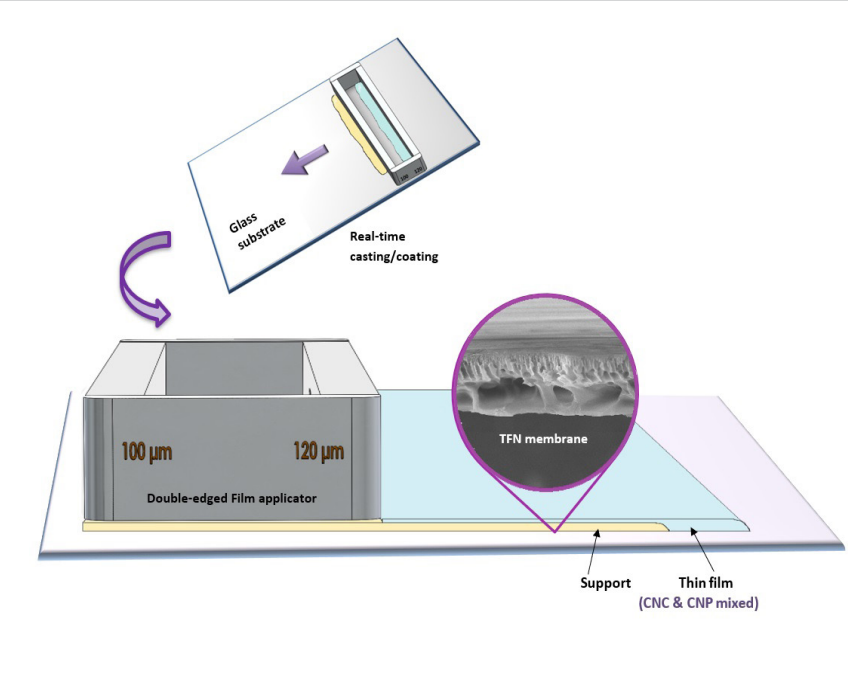

Abstract

Polyethersulfone thin film nanocomposite membrane was prepared via an innovative real-time casting-coating (RTCC) method. The formation of thin film embedded by nano-additives was along with casting the sublayer with the aid of a specialized casting knife. The current work aimed to prepare a thin layer on the membrane containing chitosan and cellulose nanocrystal nanofillers to compare the TFN PES membrane performance with mixed matrix ones. The permselectivity toward colored water by acid orange 7 (AO) and methylene blue (MB) dyes, as well as the morphological investigation of prepared membranes, were used to examine the applicability of the suggested RTCC method. Based on the results the CNC-modified membranes casted via RTCC method offered higher water flux and dye removal. Also, chitosan nanoparticles would be more efficient additives for PES membranes when they were mixed with a top-layer casting solution instead of whole membrane bulk. Significantly higher water flux (around 2 fold) and dye removal confirmed the preference for the introduced method of RTCC to prepare TFN membranes for efficient nanofiltration uses.

1. Introduction

Increasing desires of humane to synthetic products have resulted in more and more environmental pollution including water pollution by various contaminants like heavy metals, dye and pigments, drugs, etc. Dyes are one of the most used compounds in the industries and at the same time, they are the important water pollutants. Yearly, around 700000 tons of various dyes are produced for textile, paper, plastic, leather, food, and many other industries [1]. Colored wastewater can seriously harm the environment and mankind's health by being carcinogenic or allergenic [2]. However, these compounds can be

* Corresponding author: parisa_daraey@yahoo.com; p.daraei@kut.ac.ir (P. Daraei)

DOI: 10.22079/JMSR.2023.2001780.1609

removed from wastewater considering the worldwide water shortage. The treatment methods like oxidation of organic compounds, adsorption, irradiation, ion exchange, coagulation, enzyme degradation, liquid membranes, and so on are commonly used to remove dyes from water [3-11]. Most of these methods are limited by creating secondary waste which needs to be retreated, high cost, and low removal capacity [1]. Hence, the membrane filtration methods including nanofiltration and especially newly attended thin film composite (TFC) membranes are considered as a suitable treatment method [12-15]. Also, TFN membranes are very versatile tools in the water treatment process because of their high permeability and selectivity. TFN membranes have a thin active layer composed of functional nanofillers which enhance the membrane performance by creating nano-pores and changing chemical properties of this layer. The removal mechanism in TFN membranes mostly involves size exclusion, electrostatic rejection, and adsorption [16,17]. These membranes have enormous variety on account of the thin film properties, the support layer, and the method of preparing the thin film. There are different techniques to form the thin layer and improve it for enhancing the membrane flux, antifouling property, selectivity, and durability. Some examples are adding nanofillers like TiO_2, zeolites, clay, carbon nanotube, metal-organic frameworks (MOF), biopolymer nanomaterials (cellulose nanocrystal (CNC) and chitosan nanoparticles (CNP)), and etc. [18-23]. The mentioned additives are selected based on inducing the different improving properties such as hydrophilicity, antifouling capability, functional groups, and biological properties [22,23]. However, being environmentally benign and biodegradable, the biomaterials including CNC and CNP have been attracted an especial attention in preparing the mixed matrix and TFN membranes [21,22 24,25].

Employing the adsorbents in membrane preparation to uptake the contaminants has been studied many times [19,23,26]. Chitosan and its derivatives as well as cellulose are of the superior choices as the nontoxic, biodegradable, and low-cost additives [27-29]. In the previous studies, both CNC and CNP were added to the PES membrane matrices to improve the selectivity of dyes and salts [22,23]. The membranes mixed with CNC showed interesting high flux, salt and dye removal, and ultra-antifouling capability with a 99% flux recovery ratio by a simple rinsing step [22]. Application of these additives can be concluded even better results if their unique properties along with the advantages of TFNs participate in the improvement of polymeric membranes.

As mentioned before, there are different methods to deposit the thin layer on the membrane support. In the current work, the idea of preparing TFN membranes containing nanofillers (CNC and CNP) via a physical method and based on designing a special film applicator was developed. In fact, a simultaneous membrane casting and formation of thin film so-called real-time casting/coating (RTCC) method is followed in this idea. From the literature, partially similar methods of using a double-blade casting of the polymeric membrane were reported for different uses [30,31]. The recent studies used two polymer solutions with different polymer content and verified some morphological changes compared with single-blade casting. However, the current study would deeply develop the idea to investigate the capability of RTCC for the fabrication of double-layer TFN membranes using a versatile technique. In the end, it would be possible to compare the new results with the previous ones [22,23] in which the nano-additive was added into the membrane matrix and nonsolvent bath, respectively. The performance and morphology of the prepared membranes were examined. Aqueous solutions of two cationic and anionic dyes i.e. MB and AO were used as feed to be filtered using the prepared membranes. The membrane cross-sections were investigated via SEM. Also, the surface hydrophilicity, mean pore size and bulk porosity were determined.

2. Materials and methods

2.1. Chemicals

The information on all the applied chemicals is tabulated in Table 1. Distilled water was used where applicable. Demineralized water was used to prepare CNC.

2.2. CNC and CNP preparation

CNC aqueous suspension was prepared exactly the same as the previous work [22] with a size range of 100-300 nm (mean size 148 nm) confirmed by zeta sizer. Briefly, CNC was synthesized by mixing microcrystal cellulose sulfuric acid (64 wt.%) at 40°C. After diluting the suspension five times with deionized water (DI) and centrifuging the suspension for 10 min the CNCs were washed with DI water. Then, a dialysis tube was employed to remove the free acid. The solvent exchange was applied to transfer the prepared CNC from water to DMAc. For this purpose, the obtained aqueous suspension was centrifuged for 10 min at 6000 rpm, the upper water was discharged and DMAc was displaced within 5 times repeating the same procedure. As reported in previous work [23], the final content of CNC in DMAc was 0.7 wt.%). CS nanoparticles were also obtained as previous work using a repeated method in the literature [32,33]. In summary, CS powder was dissolved in 1 wt.%) acetic acid solution, and the CS nanospheres were created by dropwise addition of TPP solution into the CS solution. This method resulted in CNP with a mean size of around 120-140 nm [23].

2.3. Design of double-edge film applicator

The idea of preparation of a flat sheet polymeric membrane with two layers composed of a support layer and the functional thin top layer via a real-time casting/coating method needed a special film applicator. This applicator must have two edges with different applied thicknesses.

As depicted in Fig. 1, the manufactured film applicator has two blades with a 100 and 120 μm gap from the reliance level when located on a flat surface. This means that each blade can cast polymer solution with different thicknesses and a double-layered film can be created if polymer solution is poured in front of both blades simultaneously. Fig. 1 clearly shows the explained idea.

In this method, it is necessary to consider the correct way that the film applicator is placed on the substrate.

According to Fig. 1a, a 100 μm edge must be in front. Therefore, a double-layered film is produced with just one molding. Fig. 1b suggests the scheme of casted double-layer polymeric film on a glass substrate.

2.4. TFN membrane preparation

PES flat sheet membranes can be prepared via the phase inversion precipitation method [34]. Casting solutions with the detailed content listed in Table 2 were prepared first. The components of each casting solution were poured into individual glass vials and then mixed using a magnetic stirrer at room temperature. 24 h stirring would guarantee the homogeneity of the resulting polymer solution. In the next step, the solutions were rested for 12 h to help remove the air bubbles. Also, 15 min sonication was carried out for each solution before the casting process to ensure the bubble-free and homogeneous casting solution.

Table 1
The details of the applied chemicals.

Chemical	Supplier	Details	Pretreatment	Application
PES	BASF, Germany	Mw=58000 g/mol	No	Membrane polymer
PVP	Merck, Germany	Mw=25000 g/mol	No	Pore former
DMAc	Merck, Germany	Analytical grade	No	Polymer Solvent
AO	Merck, Germany	Analytical grade	No	Water Contaminant
MB	Merck, Germany	Analytical grade	No	Water Contaminant
Acetic Acid	Dr. Mojallali, Iran	Analytical grade	Diluted to 1 wt.%)	Chitosan solvent
Sulfuric acid	Merck, Germany	Analytical grade	Diluted to 64 wt.%)	CNC preparation
Cellulose Micro Crystals	FMC Biopolymers, Ireland	-	No	CNC preparation
Sodium tripolyohosphate (TPP)	Merck, Germany	Analytical grade	No	CNP preparation
Chitosan (CS)	Sigma-Aldrich	Low molecular weight	No	CNP preparation

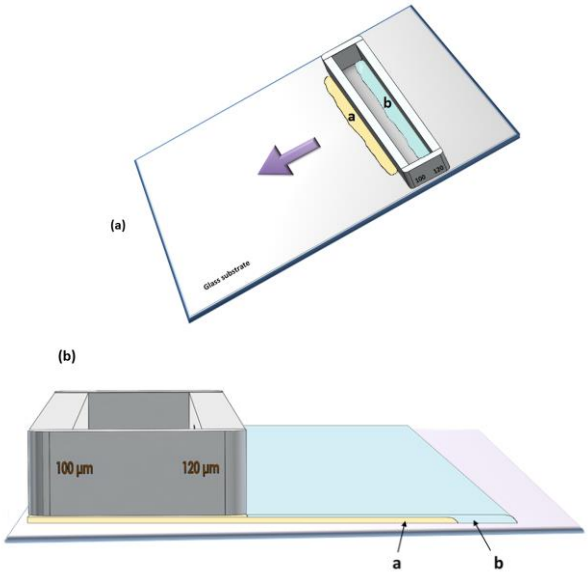

Fig. 1. a) The idea of the simultaneous casting of two different polymer solutions a and b. b) Scheme of casted double-layer polymeric film on a glass substrate

For preparing a double-layered membrane, two casting solutions were cast as described in the previous section. The casted films immediately were transferred into the non-solvent bath which contained distilled water at 20°C. The membranes rapidly precipitated and were dipped in fresh distilled water for 24 h. This helps complete the phase inversion process and extraction of water-soluble components. The coded name of each casting solution is introduced in Table 2. CNC mixed membranes were examined comprehensively and a single CNP mixed casting solution (named CS) also was prepared to compare the effects of another well-known hydrophilic nanofiller. S1 and S2 were used as a support layer and freestanding control membranes and the CNC containing S3 and S4 were cast in both forms i.e. free standing and as the thin layer on S1 and S2 supports. S4 was prepared without pore former agent (PVP) and with a high concentration of PES to investigate the effect of denser thin film on TFN membrane performance and morphology. Therefore, the prepared membranes were according to the coded names of Table 3.

Table 2
Prepared casting solution names and compositions

Membrane names	PES (wt.%)	PVP (wt.%)	Nanofiller (wt.%)	DMAc (wt.%)
S1	18	1	0	81
S2	16	2	0	82
S3	18	1	0.6 CNC	80.4
S4	20	0	0.6 CNC	79.4
CS	18	1	0.5 CNP	81

Table 3
Coded names of the prepared membranes

Membrane names	Free-standing	Support	Thin layer
S1	yes	-	-
S2	yes	-	-
S3	yes	-	-
S4	yes	-	-
S1-3	No	S1	S3
S2-3	No	S2	S3
S1-4	No	S1	S4
Cs	Yes	-	-
S1CS	No	S1	CS
S2CS	No	S2	CS

2.5. Characterization methods

In order to seek the morphological changes in the prepared membranes, SEM microphotographs of membrane cross-sections prepared by cutting in liquid N_2 were compared. A Seron (South Korea) SEM apparatus was used for imaging. Measuring the skin layer was conducted using both image analyzer software (Image J) and the live view of the membrane cross-section during the scanning. At least, 3 points were selected to be measured.

The membrane performances were evaluated by filtration test in a dead-end stirred membrane cell with 200 ml volume. Compressed air was employed to produce the needed pressure for pressure-driven membrane filtration. Each membrane sheet was firstly compressed for 10 min at 5 bar and then the pressure was descended to 4.5 bar to begin the filtration. Pure water and colored water with AO and MB dyes were applied to be passed through the membrane samples.

In this way, the pure water flux (PWF), dye removal, and permeated water flux were measured. To obtain the data, the weight and dye concentration of permeate were determined within a certain time interval for 2 h. Spectrophotometric determination of dye concentration was carried out to obtain the dye removal. Eq. 1 and 2 show the data and formulas needed for the calculation of flux and removal present:

$$\text{Flux} = \frac{M}{A \times t} \tag{1}$$

$$\text{Removal (\%)} = \left(1 - \frac{Cp}{Cf}\right) \times 100 \tag{2}$$

In these equations, M is the mass of permeate (kg), A is the membrane exposure area (19.6 cm^2), t is the time that the permeated water is collected within it (h), and C_p and C_f are the contaminant concentration in permeate and feed, respectively. It should be declared that the colored feeds were prepared by dissolving MB and AO dye in distilled water with 10 and 100 mg/L concentration, respectively. MB has a very deep blue color which makes it suitable for working at very low concentrations to investigate the membrane performance in moderately contaminated waters.

Also, there are some important characteristics of membranes like WCA and porosity which are useful for the justification of observations and should be determined. For this purpose, very small droplets of distilled water were dropped on the various random points of membranes and their contact angle was measured on the captured snapshots of droplets taken by a digital camera (2.0 Mega Pixel Color Video Camera, 500X, China) right after dropping. Image J freeware was applied for the measurements on the snapshots.

Membrane porosity can be estimated via the gravimetric method in which the volume of the penetrated water into the membrane pores within 24 h of immersion of membrane pieces in distilled water [35]. By measuring the membranes' dry and wet weight and having the membrane mean thickness and surface area (i.e. membrane volume), the determination of trapped water can be calculated. The porosity quantities can be used for estimation of membrane mean pore size via the following formula [36]:

$$\text{Mean Pore Size} = \left(\frac{(2.9 - 1.75 \times \varepsilon) \times 8 \times \eta \times L \times Q'}{\varepsilon \times A \times \Delta P}\right)^{0.5} \tag{3}$$

where, ε is the calculated porosity (%), η is the water viscosity (8.9×10^{-4} Pa.s), L is membrane thickness, Q' is the volumetric flow rate through the membrane (m^3/s), A is the membrane effective surface area (m^2) and ΔP is the trans-membrane pressure (Pa).

The measurements were all repeatedly conducted to decrease the probable inaccuracies.

3. Results and discussion

3.1. Permeability and dye removal efficiency

3.1.1. Pure water flux

When the mass of pure water passed through the membranes is investigated, it can simply show the morphological changes both in membrane bulk and surface. Fig. 2 confirms the significant alterations in membrane water permeability for pristine, mixed matrix, and TFN membranes. Firstly, the higher water flux of S2 compared to S1 was predictable because of the lower PES content of the S2 membrane which inherently results in a more porous

membrane structure. Fig. 3a compares a cross-sectional view of the prepared membranes. Increasing the membrane porosity can be clearly seen in the S2 membrane in comparison with S1. These two microphotographs i.e. S1 and S2 give a good sight of decreasing/increasing the bulk porosity as well as the skin-layer variations in the SEM images.

S1 and S3 membranes are different only in having 0.6% CNC and the related water fluxes confirm the positive effect of CNCs on membrane permeability (confirmed also in previous work [22]). Investigation of SEM images proves increasing straight finger-like cavities in the membrane sublayer for the S3 membrane compared with S1. Although the casting thickness was fixed at 120 μm for all the membranes i.e. single and double-layered ones as shown in Fig.1, the resultant membranes had thicknesses between 90- 120 μm based on the percent of shrinkage during phase inversion. Therefore, the observed permeability values are affected by the sublayer porosity and skin layer thickness rather than the membrane total thicknesses. Moreover, the hydrophilicity of S3 is higher than that of S1 based on the data in Table 4. This can be explained by the hydrophilicity of CNC which induces higher wettability to the PES membrane when mixed into the matrix [22].

In the S4 membrane, a sharp decrease of flux is obtained which undoubtedly is related to the lake of pore former. This confirms that CNC nanofiller cannot improve porosity alone however the hydrophilicity is high for this membrane. It can be concluded that porosity plays a key role in membrane permeability.

After, the interpretation of flux changes in free-standing membranes, it is more important to go through the results of TFN membranes to see whether the suggested method for preparing a double-layered polymeric membrane sounds practical or not. Actually, the free-standing S3 and S4 membranes are the control membranes to be compared with S1-3, S2-3, and S1-4. Firstly, there is no doubt that the presence of CNC either mixed with the whole membrane (S3) or mixed only in the top layer (S1-3 and S2-3) can increase the membrane porosity, hydrophilicity, and water flux. The data in Table 4 confirms this statement. Therefore, both S1-3 and S3 offered higher flux (141.4 and 112 $kg.m^{-2}.h^{-1}$) relative to S1 (102.3 $kg.m^{-2}.h^{-1}$). Similarly, S2-3 is more permeable than S2 and also S3. This is evidence that the double-layered (TFN) membrane can have higher water flux. The similar contact angle results for S3, S1-3, and S2-3 verify that mixing hydrophilic filler into the top layer of the membrane can be replaced by adding them into the whole membrane matrix. This can effectively reduce nanofiller consumption and costs.

The parameter that had the most significant change for the TFN membranes is the skin-layer thickness which is sensibly decreased for S1-3 and S2-3. Comparing S1-3 with S2-3 can declare the effect of support layer density on TFN membrane permeability. Decreasing the polymer content, from 18 wt.% in S1 to 16 wt.% in S2, resulted in higher permeability in S2-3 which used S2 as support. Hence, in preparing the double-layered membranes via RTCC method the permeability can be increased by decreasing the sublayer polymer content to an optimum amount. Of course, permeability would be worthy along with effective selectivity. So, the dye removal results must be considered for the conclusion. The effect of double-layered casting in permeability is to some extent that even S1-4 showed extremely higher flux relative to S4. In this membrane, the undesirable effect of not using pore former in membrane preparation has been effectively compensated by applying a porous sublayer.

SEM images show different morphology for TFN membranes (S1-3 and S2-3) compared with free-standing S1, S2, and S3. It seems that the integrity of the pores has disappeared in TFN membranes and the sub-layer macrovoid shapes have been changed from vertical ovals for free-standing membranes to horizontally lying voids for TFN ones. This might be due to the shear stress that the upper casting solution exerted on the lower one during the casting process. It is obvious in Fig. 2 b that the upper polymer solution (b) is cast on the lower one (a). This can dislocate the solution in the interface layer before membrane precipitation in the non-solvent bath.

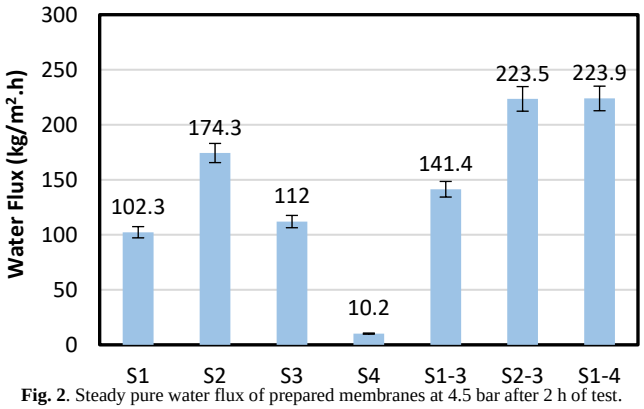

Fig. 2. Steady pure water flux of prepared membranes at 4.5 bar after 2 h of test.

3.1.2. Dye removal ability

Dye removal percent and permeate flux for CNC-modified membranes are demonstrated in Fig 4 The results showed that dye removal for the membranes containing CNC is significantly higher compared to S1 and S2 confirming the previous results [22]. According to the dye removal data, both AO and MB dyes were differently removed by S3, S1-3, S2-3, and S1-4 membranes. Generally, the superior dye removal is attributed to TFN membranes. However, some different results are achieved for S2-3 which need discussion.

The molecular weight of MB (350.3 g/mol) is greater than that of AO (319.8 g/mol). Then, it is predicted that MB molecules be larger and a sieving mechanism will run to remove this dye. Also, the results of dye removal for S1 and S2 verify a sieving mechanism because the removal of MB is greater than AO for the pristine membranes. However, in CNC-containing membranes, the removal of AO is greater than MB (except for S4) which verifies the other retention mechanism cooperating with the sieving mechanism.

The surface charge of CNC has been reported to be negative before [22, 37]. Hence, it is expected that by the addition of CNC into the membranes their surface charge gets negative as well [22]. Since AO is an anionic dye, the negative charge of dye molecules is repelled by the negative charge of the membrane surface. The S4 membrane is very dense because of lacking pore former and sieving is the dominant removal mechanism all the time.

The effects of changes on the membrane surface charge can also be observed in permeate flux results depicted in Fig. 4. In general, the repulsion of the species charged the same as the membrane surface leads to facilitated passage of water through the membrane. On the contrary, the oppositely charged molecules are adsorbed by the membrane surface and this can decrease the membrane flux as a result of surface pore blockage and decrease the number of pores [12]. Therefore, the positive MB adsorbed onto the negatively charged PES membrane. By adsorption of dye on the membrane surface, the membrane surface pore blockage was expected; however, the flux decline is limited in CNC-containing membranes due to higher hydrophilicity and thinner skin layer. CNC in the membrane can affect the membrane mean pore sizes according to the data in Table 4. The mean pore size is smaller in CNC-improved membranes, especially in double-layered TFN membranes. Decreasing the mean pore size can help better the sieving mechanism, and TFN membranes are even more effective from this point of view.

Table 4
Prepared membrane main characteristics.

Membrane	S1	S2	S3	S4	S1-3	S2-3	S1-4
ε (%)	45±2	90±2	82±2	39±2	91±3	86±3	81±2
WCA (°)	67.4±2.1	66.5±3.5	55.2±1.6	54±2.1	55.1±1.2	54.9±2.6	52.6±2.3
Skin-layer Thickness (μm)	2.2±0.2	2.0±0.2	1.2±0.3	0.9±0.1	0.8±0.2	0.6±0.1	0.7±0.1
ε (%) with Image J	44±2	89±2	79±3	38±2	92±5	88±3	83±3
Mean Pore Size (nm)	20.5	21.2	15.7	13.2	10.5	11.3	10.1

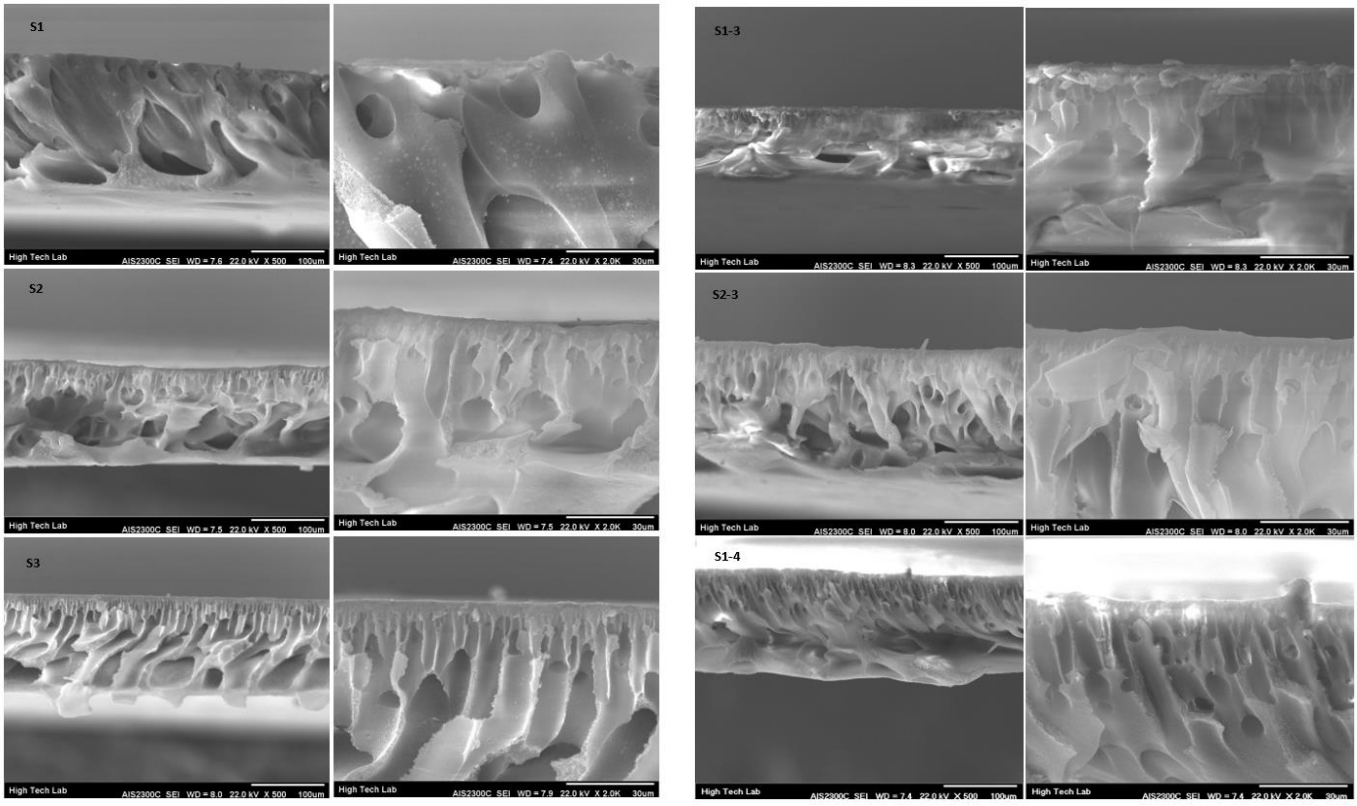

(a)

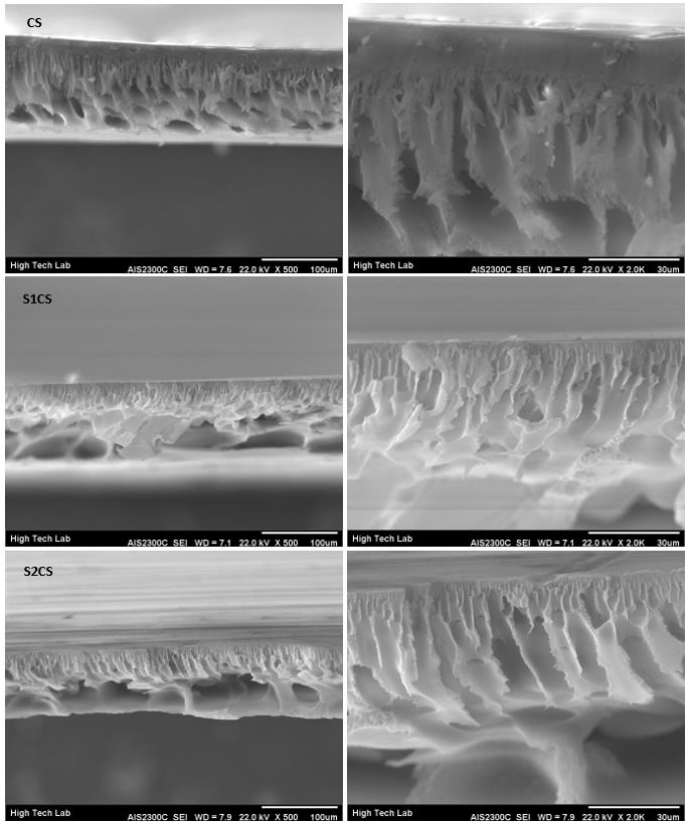

(b)

Fig. 3. a) Cross-section view of free-standing and TFN membranes filled with CNC recorded by SEM apparatus at two different magnifications, 500X left and 2000X right, b) SEM images of CS-modified membranes comparing free-standing and double-layered membranes.

As a general conclusion, this investigation proved that only small amounts of an additive like CNC in the top layer of a double-layered membrane prepared by a novel RTCC method can result in more preferred results in removing dye from water. The result of this work compared with the previous work on the common mixed matrix membrane [22] showed about 15% higher dye removal and four-fold higher water flux. Besides, all the prepared membranes were stable and did not crash during the tests. Therefore, it can be claimed that the preparation method did not influence the membrane mechanical resistance within the tested range of trans-membrane pressure which matches with nanofiltration common process pressure. The thermal and chemical stability couldn't be influenced as well because the membrane material was unchanged and only the use of nanofiller was optimized by adding it to the top layer instead of the whole membrane matrix. However, the new casting/coating method needs more investigation.

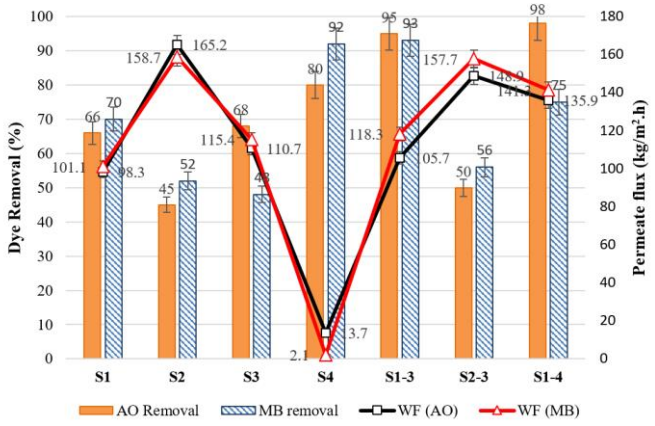

Fig. 4. AO and MB dye removal from aqueous feed solution calculated and permeate flux for control and CNC-improved TFN membranes after 2 h of test beginning.

3.1.3. Trying RTCC for CNP nanofiller

According to the results of testing RTCC in adding CNC to the PES membrane top layer, there would be stronger evidence if the other pretested nanofiller was examined. As embedding CNP into PES has been reported to offer perfect results in improving the PES membrane, this nanofiller was selected to be tested in the RTCC method. Therefore, the membranes with coded names of CS, S1CS, and S2CS in Table 2 were fabricated. The water flux and AO dye removal were determined for this group of membranes. For this purpose, the process was repeated for these membranes exactly similar to the previous part of the experiments. 100 mg/l AO solution was used as feed. Table 5 offers pure water flux as well as the permeated water flux for CNP-modified membranes to compare the free-standing CS membrane with two double-layered TFN membranes.

Based on the results, the permeability of double-layered membranes is much higher than free-standing ones. As it is known, the membrane flux is affected by its skin-layer thickness, surface hydrophilicity, pore radius, and porosity. Hence, all these parameters were determined for the prepared membranes (Table 5).

The morphological data in Table 5 were all achieved from SEM images depicted in Fig. 3b. It is crystal clear that the membrane porosity of TFN membranes increased significantly. This is due to the sublayer big macrovoids which are visible in SEM images of S1CS and S2CS membranes.

Table 5
Membrane characteristics for CNP-modified membranes.

Membrane	CS	S1CS	S2CS
ε (%)	67	92	89
WCA (°)	54.8	52.3	53.1
Skin-layer Thickness (μm)	0.93	0.62	0.55
Mean Pore Size (nm)	12.9	10.3	9.9
PWF ($kg.m^{-2}.h^{-1}$)	121.4	220.9	185.1
Permeate flux ($kg.m^{-2}.h^{-1}$)	91.5	153.2	127.4
AO removal (%)	72	96	69

As it is expected there is no significant change in membrane hydrophilicity because they all contain the same CNP. However, the WCA sensibly decreased relative to S1 and S2 pristine membranes as a result of blended hydrophilic CNP in the membrane matrix and top layer.

Absolutely, the membrane's high flux is worth it if the selectivity remains unchanged or even improves. The AO dye removal results are represented in Table 5.

CS particles are uncharged at neutral pHs [23]. Then, the removal of dye molecules with a negative charge cannot be attributed to the electrostatic repulsion. Instead, CS has an intrinsic adsorption ability and is assumed as an adsorptive material [23, 27]. Therefore, dye removal by Cs-modified membranes can be adsorbed on the modified membrane. This is supposed to block the membrane pores and decline the permeability but the flux of CS-modified membranes is still higher than S1 and S2. Again, membrane hydrophilicity, high porosity, and thin skin layer promoted the water permeability. Comparing the results for S1CS and S2CS membranes offers that applying same PES content for two layers gives better result in the case of AO removal. Actually, S2CS membrane has PES 16% as its sublayer which makes different morphology relative to S1CS membrane. The lower permeability along with lower dye removal percent of S2CS might be a sign for more serious mixing of two layers during casting process which is logical because of higher content of solvent (DMAc) in sub-layer. The increased mixing of two layer interfaces can decrease the content of CNP in top-layer and diminish the dye removal as a result. Instead, the absorbed dye molecules in inner pores make the membrane less permeable to the water as the lower flux of S2CS implies.

CS was an effective additive in previous work [23] but could be even more improved when the membrane was cast in double-layer form using the RTCC method.

4. Comparison of the study results

CNCs have been progressively used for contamination removal from aqueous solutions. Table 6 summarizes a comparison of the efficiency of CNC-improved membranes for removing various types of contaminants from water. Based on the reports, the current study achieved acceptable performance of CNC-modified membrane via fabrication of TFN membrane with the suggested RTCC method.

Also, the literature review confirms that dual-layered membranes apart from the preparation technique and the layers' main material widely used for the fabrication of high-performance polymeric membranes as listed in Table 7. According to the information in Table 7, the RTCC method of preparing TFN membrane in this study is well performed compared with other methods of dual-layered membrane preparation.

Table 6
Comparison of the removal result of this study with some other different membranes that have CNCs in their structures.

Contaminant	Membrane modifier	Removal (%)	Ref.
MB AO	CNC (in TFN)	93 98	This study
AO	CNC (mixed matrix membrane)	79.1	[22]
BSA protein	CNC (mixed matrix)	99	[25]
Copper ions	l-cysteine functionalized CNC (mixed matrix)	98.4	[38]
Congo Red	Polydopamine-modified CNC (mixed matrix)	99.9	[39]
Nitrate	Sawdust-derived CNC (mixed matrix)	94	[40]

Table 7
High-performance dual-layered membranes in dye and organic material removal.

Contaminant	Membrane layers (main material)	Removal (%)	Ref.
Congo Red	Covalent organic framework/MXene	99.6	[41]
Blue dextran	Cu_2O/PVDF	75	[42]
Bisphenol-A	Polyethylene-imine grafted on polyamide	98.5 46.2	[43]
MB	Oxidized and polyethyleneimine functionalized MWCNT	99.9	[44]

5. Conclusion

The feasibility of using the novel RTCC method in the preparation of TFN membranes containing CNC and CNP was investigated. The efficiency of the introduced method was examined via membrane permselectivity test and the results were justified with the aid of characterization analysis including SEM, WCA, mean pore size, and porosity. Based on the results, the CNC-containing membranes exhibited significantly higher water flux and dye removal (98% of AO and 93% MB) when cast via the RTCC method. In fact, the porous sub-layer and the functional top-layer cooperated to enhance both permeability and selectivity. However, it is necessary to test more pretested nano-additives to better conclude the effectiveness of the RTCC method.

As the next step, CNP was examined in the same way to confirm the preference of RTCC for single-layer casting of common mixed matrix membranes. The results were improved for the double-layered CS-modified membranes compared with the simple mixed matrix one. Higher AO removal along with higher flux was achieved similar to the CNC-modified double-layered membranes.

Overall, it can be a preliminary conclusion that the new RTCC method can result in a different performance of the membrane compared with the freestanding membrane with the same composition. At the same time, RTCC can decrease nanofiller consumption. Most importantly, the method can be further explored with various casting solutions containing different polymers and even different solvents.

Acknowledgment

The authors would like to acknowledge the financial support of Kermanshah University of Technology for this research under grant number S/P/T/1164.

CRedit authorship contribution statement

P. Daraei: Data curation; Formal analysis; Supervision; Writing – review & editing.
K. Rostami: Investigation; Methodology.
F. Nasirmanesh: Conceptualization; Validation; Visualization; Writing – original draft.

Funding sources

This research received financial support from Kermanshah University of Technology under grant number S/P/T/1164.

Declaration of Competing Interest

The authors declare that they have no known competing financial interests or personal relationships that could have appeared to influence the work reported in this paper.

Data availability

Data are available upon request.

References

[1] V. Katheresan, J. Kansedo, S.Y. Lau, Efficiency of various recent wastewater dye removal methods: A review, J. Environ. Chem. Eng., 6 (2018) 4676-4697. https://doi.org/10.1016/j.jece.2018.06.060.
[2] A.Y. Tang, C.K. Lo, C.w. Kan, Textile dyes and human health: A systematic and citation network analysis review, Color. Technol., 134 (2018) 245-257. https://doi.org/10.1111/cote.12331
[3] A. Shoiful, H. Kambara, L.T.T. Cao, S. Matsushita, T. Kindaichi, Y. Aoi, N. Ozaki, A. Ohashi, Mn (II) oxidation and manganese-oxide reduction on the decolorization of an azo dye, Int. Biodeterior. Biodegradation, 146 (2020) 104820. https://doi.org/10.1016/j.ibiod.2019.104820
[4] R. Shokoohi, M. Salari, R. Safari, H. Zolghadr Nasab, S. Shanehsaz, Modelling and optimisation of catalytic ozonation process assisted by ZrO2-pumice/H2O2 in the degradation of Rhodamine B dye from aqueous environment, Int J. Environ. Anal. Chem., (2020) 1-25. https://doi.org/10.1080/03067319.2019.1704748
[5] S. Dawood, T.K. Sen, C. Phan, Performance and dynamic modelling of biochar and kaolin packed bed adsorption column for aqueous phase methylene blue (MB) dye removal, Environ. Technol., (2018). https://doi.org/10.1080/09593330.2018.1491065
[6] D. D'Angelo, S. Filice, A. Scarangella, D. Iannazzo, G. Compagnini, S. Scalese, Bi2O3/Nexar® polymer nanocomposite membranes for azo dyes removal by UV–vis or visible light irradiation, Catal. Today, 321 (2019) 158-163. https://doi.org/10.1016/j.cattod.2017.12.013
[7] V. Kumar, Adsorption kinetics and isotherms for the removal of rhodamine B dye and Pb+ 2 ions from aqueous solutions by a hybrid ion-exchanger, Arab. J. Chem., 12 (2019) 316-329. https://doi.org/10.1016/j.arabjc.2016.11.009
[8] K. Bahrpaima, P. Fatehi, Preparation and coagulation performance of carboxypropylated and carboxypentylated lignosulfonates for dye removal, Biomolecules, 9 (2019) 383. https://doi.org/10.3390/biom9080383
[9] E. Bahadori, M. Rapf, A. Di Michele, I. Rossetti, Photochemical vs. photocatalytic azo-dye removal in a pilot free-surface reactor: Is the catalyst effective?, Sep. Purif. Technol., 237 (2020) 116320. https://doi.org/10.1016/j.seppur.2019.116320
[10] W. Chen, J. Mo, X. Du, Z. Zhang, W. Zhang, Biomimetic dynamic membrane for aquatic dye removal, Water Res., 151 (2019) 243-251. https://doi.org/10.1016/j.watres.2018.11.078
[11] A. Shokri, P. Daraei, S. Zereshki, Water decolorization using waste cooking oil: An optimized green emulsion liquid membrane by RSM, J. Water Process. Eng., 33 (2020) 101021. https://doi.org/10.1016/j.jwpe.2019.101021
[12] N. Ghaemi, P. Safari, Nano-porous SAPO-34 enhanced thin-film nanocomposite polymeric membrane: simultaneously high water permeation and complete removal of cationic/anionic dyes from water, J. Hazard. Mater., 358 (2018) 376-388. https://doi.org/10.1016/j.jhazmat.2018.07.017
[13] Y. Wu, M. Gao, W. Chen, Z. Lü, S. Yu, M. Liu, C. Gao, Efficient removal of anionic dye by constructing thin-film composite membrane with high perm-selectivity and improved anti-dye-deposition property, Desalination, 476 (2020) 114228. https://doi.org/10.1016/j.desal.2019.114228
[14] D. Wu, X. Zhang, Y. Chen, S. Yu, H. Zhao, Thin film composite polyesteramide nanofiltration membranes fabricated from carboxylated chitosan and trimesoyl chloride, Korean J. Chem. Eng., 37 (2020) 307-321. https://doi.org/10.1007/s11814-019-0426-4
[15] Q. Li, Z. Liao, X. Fang, J. Xie, L. Ni, D. Wang, J. Qi, X. Sun, L. Wang, J. Li, Tannic acid assisted interfacial polymerization based loose thin-film composite NF membrane for dye/salt separation, Desalination, 479 (2020) 114343. https://doi.org/10.1016/j.desal.2020.114343
[16] L.-x. Dong, X.-c. Huang, Z. Wang, Z. Yang, X.-m. Wang, C.Y. Tang, A thin-film nanocomposite nanofiltration membrane prepared on a support with in situ embedded zeolite nanoparticles, Sep. Purif. Technol., 166 (2016) 230-239. https://doi.org/10.1016/j.seppur.2016.04.043
[17] J. Zhu, M. Tian, Y. Zhang, H. Zhang, J. Liu, Fabrication of a novel "loose" nanofiltration membrane by facile blending with Chitosan–Montmorillonite nanosheets for dyes purification, J. Chem. Eng., 265 (2015) 184-193. https://doi.org/10.1016/j.cej.2014.12.054
[18] H. Chen, M. Huang, Z. Wang, P. Gao, T. Cai, J. Song, Y. Zhang, L. Meng, Enhancing rejection performance of tetracycline resistance genes by a TiO2/AgNPs-modified nanofiber forward osmosis membrane, Chem. Eng. J., 382 (2020) 123052. https://doi.org/10.1016/j.cej.2019.123052
[19] S.R. Mousavi, M. Asghari, N.M. Mahmoodi, Chitosan-wrapped multiwalled carbon nanotube as filler within PEBA thin film nanocomposite (TFN) membrane to improve dye removal, Carbohydr. Polym., 237 (2020) 116128. https://doi.org/10.1016/j.carbpol.2020.116128
[20] M.M. Baneshi, A.M. Ghaedi, A. Vafaei, D. Emadzadeh, W.J. Lau, H. Marioryad, A. Jamshidi, A high-flux P84 polyimide mixed matrix membranes incorporated with cadmium-based metal-organic frameworks for enhanced simultaneous dyes removal: response surface methodology, Environ. Res., 183 (2020) 109278. https://doi.org/10.1016/j.envres.2020.109278
[21] P. Daraei, N. Ghaemi, H.S. Ghari, M. Norouzi, Mitigation of fouling of polyethersulfone membranes using an aqueous suspension of cellulose nanocrystals as a nonsolvent, Cellulose, 23 (2016) 2025-2037. https://doi.org/10.1007/s10570-016-0937-7
[22] P. Daraei, N. Ghaemi, H.S. Ghari, An ultra-antifouling polyethersulfone membrane embedded with cellulose nanocrystals for improved dye and salt removal from water, Cellulose, 24 (2017) 915-929. http://dx.doi.org/10.1007/s10570-016-1135-3
[23] N. Ghaemi, P. Daraei, F.S. Akhlaghi, Polyethersulfone nanofiltration membrane-embedded by chitosan nanoparticles: Fabrication,

characterization, and performance in nitrate removal from water, Carbohydr. Polym., 191 (2018) 142-151. https://doi.org/10.1016/j.carbpol.2018.03.024
[24] Z. Karim, A.P. Mathew, M. Grahn, J. Mouzon, K. Oksman, Nanoporous membranes with cellulose nanocrystals as functional entity in chitosan: removal of dyes from water, Carbohydr. Polym., 112 (2014) 668-676. https://doi.org/10.1016/j.carbpol.2014.06.048
[25] H. Bai, X. Wang, H. Sun, L. Zhang, Permeability and morphology study of polysulfone composite membrane blended with nanocrystalline cellulose, Desalin. Water Treat., 53 (2015) 2882-2896. https://doi.org/10.1080/19443994.2013.875944
[26] G.I. Danmaliki, T.A. Saleh, Effects of bimetallic Ce/Fe nanoparticles on the desulfurization of thiophenes using activated carbon, Chem. Eng. J.l, 307 (2017) 914-927. https://doi.org/10.1016/j.cej.2016.08.143
[27] F. Fu, Q. Wang, Removal of heavy metal ions from wastewaters: a review, J. Environ. Manage., 92 (2011) 407-418. https://doi.org/10.1016/j.jenvman.2010.11.011
[28] M. Rinaudo, Chitin and chitosan: Properties and applications, Prog. Polym. Sci., 31 (2006) 603-632. https://doi.org/10.1016/j.progpolymsci.2006.06.001
[29] M.N.R. Kumar, A review of chitin and chitosan applications, React. Funct. Polym., 46 (2000) 1-27. https://doi.org/10.1016/S1381-5148(00)00038-9
[30] Q.-C. Xia, M.-L. Liu, X.-L. Cao, Y. Wang, W. Xing, S.-P. Sun, Structure design and applications of dual-layer polymeric membranes, J. Membr. Sci., 562 (2018) 85-111. https://doi.org/10.1016/j.memsci.2018.05.033
[31] X. Liu, H.Y. Ng, Double-blade casting technique for optimizing substrate membrane in thin-film composite forward osmosis membrane fabrication, J. Membr. Sci., 469 (2014) 112-126. https://doi.org/10.1016/j.memsci.2014.06.037
[32] N. Ghaemi, S.S. Madaeni, A. Alizadeh, H. Rajabi, P. Daraei, Preparation, characterization and performance of polyethersulfone/organically modified montmorillonite nanocomposite membranes in removal of pesticides, J. Membr. Sci., 382 (2011) 135-147. https://doi.org/10.1016/j.memsci.2011.08.004
[33] X. He, M. Du, H. Li, T. Zhou, Removal of direct dyes from aqueous solution by oxidized starch cross-linked chitosan/silica hybrid membrane, Int. J. Biol. Macromol., 82 (2016) 174-181. https://doi.org/10.1016/j.ijbiomac.2015.11.005
[34] N. Ghaemi, F. Nasirmanesh, Synthesis of a hybrid organic-inorganic polyethersulfone membrane incorporated with phosphotungstic acid: controversial performance in removal of dinitroaniline herbicides from water, J. Clean. Prod., 182 (2018) 259-271. https://doi.org/10.1016/j.jclepro.2018.02.069
[35] J.-F. Li, Z.-L. Xu, H. Yang, L.-Y. Yu, M. Liu, Effect of TiO2 nanoparticles on the surface morphology and performance of microporous PES membrane, Appl. Surf. Sci., 255 (2009) 4725-4732. https://doi.org/10.1016/j.apsusc.2008.07.139
[36] N. Hamid, A. Ismail, T. Matsuura, A. Zularisam, W. Lau, E. Yuliwati, M. Abdullah, Morphological and separation performance study of polysulfone/titanium dioxide (PSF/TiO2) ultrafiltration membranes for humic acid removal, Desalination, 273 (2011) 85-92. https://doi.org/10.1016/j.desal.2010.12.052
[37] Y. Li, Y. Liu, W. Chen, Q. Wang, Y. Liu, J. Li, H. Yu, Facile extraction of cellulose nanocrystals from wood using ethanol and peroxide solvothermal pretreatment followed by ultrasonic nanofibrillation, Green Chem., 18 (2016) 1010-1018. https://doi.org/10.1039/C5GC02576A
[38] F. Abedi, M.A. Dubé, D. Emadzadeh, B. Kruczek, Improving nanofiltration performance using modified cellulose nanocrystal-based TFN membranes, J. Membr. Sci., 670 (2023) 121369. https://doi.org/10.1016/j.memsci.2023.121369
[39] L. Yang, X. Liu, X. Zhang, T. Chen, Z. Ye, M.S. Rahaman, High-performance nanocomposite nanofiltration membranes with polydopamine-modified cellulose nanocrystals for efficient dye/salt separation, Desalination, 521 (2022) 115385. https://doi.org/10.1016/j.desal.2021.115385
[40] A. Adeniyi, D. Gonzalez-Ortiz, C. Pochat-Bohatier, S. Mbakop, M.S. Onyango, Preparation of nanofiltration membrane modified with sawdust-derived cellulose nanocrystals for removal of nitrate from drinking water, Membranes, 12 (2022) 670. https://doi.org/10.3390/membranes12070670
[41] C. Feng, K. Ou, Z. Zhang, Y. Liu, Y. Huang, Z. Wang, Y. Lv, Y.-E. Miao, Y. Wang, Q. Lan, Dual-layered covalent organic framework/MXene membranes with short paths for fast water treatment, J. Membr. Sci., 658 (2022) 120761. https://doi.org/10.1016/j.memsci.2022.120761
[42] C.-C. Ho, J.F. Su, Boosting permeation and separation characteristics of polyethersulfone ultrafiltration membranes by structure modification via dual-PVP pore formers, Polymer, 241 (2022) 124560. https://doi.org/10.1016/j.polymer.2022.124560
[43] S.H. Mohamed Noor, M.H.D. Othman, W. Khongnakorn, O. Sinsamphanh, H. Abdullah, M.H. Puteh, T.A. Kurniawan, H.S. Zakria, T. El-Badawy, A.F. Ismail, Bisphenol A removal using visible light driven Cu2O/PVDF photocatalytic dual-layer hollow fiber membrane, Membranes, 12 (2022) 208. https://doi.org/10.3390/membranes12020208
[44] M.J. Huhn-Ibarra, M.I. Loría-Bastarrachea, S. Duarte-Aranda, A.d.J. Montes-Luna, J. Ortiz-Espinoza, M.O. González-Díaz, M. Aguilar-Vega, PPSU dual-layer hollow fiber mixed matrix membranes with functionalized MWCNT for enhanced antifouling, salt and dye rejection in water treatment, J. Appl. Polym. Sci., 139 (2022) e53203. https://doi.org/10.3390/membranes12020208